The effect of substrate stiffness, thickness, and cross-linking density on osteogenic cell behavior

The Effect of Substrate Stiffness, Thickness and Crosslinking Density on Osteogenic Cell Behaviour

*Mullen, C. A.[1,2], T. J. Vaughan[1], K. L. Billiar[3], L.M. McNamara[1,2]

[1] Centre for Biomechanics Research (BMEC), Department of Biomedical Engineering, NUI Galway, Ireland

[2] National Centre for Biomedical Engineering Science (NCBES), NUI Galway, Ireland

[3] Department Biomedical Engineering, Worcester Polytechnic Institute, Worcester, Massachusetts, USA

Address for correspondence:
Dr. Laoise M. McNamara
Department of Mechanical and Biomedical Engineering
National University of Ireland Galway
Galway,
Ireland
Phone: (353) 91-492251
Fax: (353) 91-563991
Email: Laoise.McNamara@nuigalway.ie

Abstract:

Osteogenic cells respond to mechanical changes in their environment by altering their spread area, morphology and gene expression profile. In particular the bulk modulus of the substrate, as well as its microstructure and thickness, can substantially alter the local stiffness experienced by the cell. Although bone tissue regeneration strategies involve culture of bone cells on various biomaterial scaffolds, which are often crosslinked to enhance their physical integrity, it is difficult to ascertain and compare the local stiffness experienced by cells cultured on different biomaterials. In this study, we seek to characterise the local stiffness at the cellular level for MC3T3-E1 cells plated on biomaterial substrates of varying modulus, thickness and crosslinking concentration. Cells were cultured on flat and wedge shaped gels made from polyacrylamide or crosslinked collagen. The crosslinking density of the collagen gels was varied to investigate the effect of fibre crosslinking in conjunction with substrate thickness. Cell spread area was used as a measure of osteogenic differentiation. Finite element simulations were used to examine the effects of fibre crosslinking and substrate thickness on the resistance of the gel to cellular forces, corresponding to the equivalent shear stiffness for the gel structure in the region directly surrounding the cell. The results of this study show that MC3T3 cells cultured on a soft fibrous substrate attain the same spread cell area as those cultured on a much higher modulus, but non-fibrous, substrate. FE simulations predict that a dramatic increase in the equivalent shear stiffness of fibrous collagen gels occurs as crosslinking density is increased, with equivalent stiffness also increasing as gel thickness is decreased. These results provide an insight into the response of osteogenic cells to individual substrate parameters and have the potential to inform future bone tissue regeneration strategies that can optimise the equivalent stiffness experienced by cell.

Introduction

Osteogenic cells possess a highly developed cytoskeleton (1, 2), and have been long regarded as efficacious mechanosensors (3, 4). There has been widespread investigation into the effect of various mechanical forces, including substrate stiffness (5, 6), fluid flow induced shear stress (7) and applied substrate strain (8) on osteogenic cell behaviour. While a general consensus exists that an understanding of mechanotransduction is necessary for the treatment of disease originating at the cellular level and the development of tissue engineering strategies (2, 9, 10), the exact nature of the methods by which cells interact with their environment must be delineated if the mechanotransduction of osteogenic cells is to be better understood. Specifically the combined effects of bulk material modulus, substrate thickness and the microstructure of the substrate have yet to be investigated.

One of the most common methods of investigating mechanotransduction is the culture of cells on substrates of controllable modulus and it has been shown that a change in substrate modulus can affect osteoblast behaviour, including proliferation, migration and differentiation (11-13). There are various approaches for altering the modulus of substrate materials for in vitro cell culture applications. Collagen, the primary component of the matrix on which bone cells develop, can be modified using a variety of crosslinking methods including chemical crosslinkers, such as glutaraldehyde and 1-Ethyl-3-(3-dimethylaminopropyl)carbodiimide (EDAC), as well as exposure to ultraviolet light to achieve a specific bulk substrate modulus (14, 15). Polyacrylamide is widely used in mechanotransduction studies due to the relative ease and reliability with which its modulus can be altered, specifically by varying the percentage of acrylamide and bis-acrylamide used in the polymerisation process (16, 17). A range of other polymers including polydimethylsiloxane (13), polyethylene glycol (18) and polymethyl methacrylate (19) have also been used as substrates of controllable modulus.

Recently, substrate thickness has been used as a method of varying the stiffness experienced by the cell (20, 21). The structural stiffness experienced by the cell is affected by both the substrate geometry, most notably the distance to the substrate boundaries (21), and the substrate modulus, an intrinsic property of the substrate material. On thin substrates (< 5 μm) cell-induced contractility forces can propagate through the entirety of the substrate allowing the mechanical properties of the underlying material, often glass coverslips or tissue culture plastic, to influence cell behaviour. However, the effect of substrate thickness is also governed by the structure of the substrate in question. Specifically it has been demonstrated that cell-induced stresses travel only a few microns through linear, homogenous substrates, such as polyacrylamide (22), while cells on fibrous substrates have been shown to be influenced by structures which are hundreds of microns away (20, 23); for example, underlying rigid coverslips have been shown to influence cell spreading and morphology on fibrous substrates of up to 130 μm thick (24). The enhanced propagation of mechanical signals has been attributed to the fibrous nature of biological substrates; specifically, it has been proposed that cell-induced forces propagate through individual fibres over long distances (24, 25).

The specific effect of fibres on the mechanical properties of fibrous gels has been investigated through computational approaches. A microscale discrete fibre representative element has been linked to a Galerkin macroscale model to study the effects of fibrosity on bulk collagen gel properties (26). This method has been further developed to investigate both fibrous wound behaviour (27) and the response of cells to gel fibrosity (24). However, this approach prevents fibres from extending across elements at the macroscopic level. In the

relatively thin (70 μm) substrates used in typical cell mechanotransduction experiments (21), collagen fibres may extend through the entire gel thickness.

The range of methods used to alter substrate stiffness experienced by the cell has led to apparent contradictions regarding the response of osteoblastic cells to their local mechanical environment. For example osteoblast differentiation has been shown to occur on collagen coated polymer substrates between 20 and 40 kPa (5, 18). Meanwhile our own previous work has shown that osteoblast differentiation occurs on type 1 collagen substrates of 1 kPa, while softer substrates of 300 Pa induce osteoblast differentiation followed by early osteocyte differentiation. Such discrepancies are likely explained by the fact that the bulk modulus of the substrate is usually reported, whereas the precise stiffness experienced by the cell, here termed the equivalent stiffness, is dictated by the material modulus, substrate thickness and substrate microstructure, which can all vary dramatically depending on the biomaterial fabrication processes (e.g. cross-linking). However, it is difficult to ascertain the equivalent stiffness experienced by the cell and as such it is not yet known precisely how each property contributes to the local mechanical stimulation of osteogenic cells. The field of bone tissue engineering has thus far relied primarily on measurement of bulk material properties to ascertain the effect of extracellular mechanical cues imparted by biomaterial scaffolds on cell differentiation. However, the effects of other ECM properties such as size and microstructure cannot be ignored and must be investigated in greater detail if the efficacy of various biomaterials in osteogenic differentiation is to be understood.

The objective of this study is to derive an understanding of the individual and combined effects of substrate modulus, fibrosity, thickness and crosslinking density on the local stiffness experienced by osteoblastic cells. MC3T3-E1 cells were cultured on flat and wedge shaped non-fibrous polyacrylamide and fibrous collagen gels, while cell spread area and ALP activity were used as early indicators of cell differentiation. Crosslinked collagen gels (of varied crosslinking density) were then used to determine the effect of fibre crosslinking in conjunction with substrate thickness on the differentiation of osteogenic cells. Finite element models were generated to represent the contraction of an osteoblastic cell on a soft linearly elastic gel with discrete tensile collagen fibres. These models were used to investigate the transfer of force through collagen gels of different crosslinking density over a range of gel thicknesses. We hypothesise that the equivalent stiffness as experienced by the cell is influenced by gel bulk stiffness, thickness and crosslinking density and that these factors must be accounted for when investigating mechanotransduction in vitro.

Methods

Experimental methods

Substrate manufacture

Flat and wedges shaped collagen gels were prepared as described previously (6). Briefly, rat tail type 1 collagen (Sigma-Aldrich, St-Louis MO) was neutralised using 10 mM NaOH, and diluted to 4 mg/mL with dH_2O. Glass slides were activated by sonicating in 1% 3-aminopropyltrimethoxy silane (Sigma-Aldrich) before being incubated in 0.5% glutaraldehyde (Sigma-Aldrich) overnight. The mixture was pipetted onto the activated glass slides (Electron Microscopy Sciences, Hatfield PA) while a cover slide, treated with Sigmacote (Sigma-Aldrich), was placed over the gel to allow the gel to set without adhering to the cover slide. Wedges shaped gels were constructed by placing a 150 μm coverslip on

one side of the glass slide, forming a wedge shaped mould within which the gel was set, as shown in Figure 1 A). Following gel formation the top coverslip was removed leaving the wedge shaped gel as shown in Figure 1 B). Flat gels were formed at approximately 70 μm thick, while wedge shaped gels ranged from 0 to 150 μm over a lateral distance of 50 mm. The modulus of collagen gels was controlled through chemical crosslinking with 1-Ethyl-3-(3-dimethylaminopropyl)carbodiimide (EDAC)/N-hydroxysulfosuccinimide (NHS) (both Sigma Aldrich), resulting in the formation of zero length crosslinks between fibres. Formed gels were treated with 0, 20, 50, 100 or 150 mM EDAC/mg collagen at a 9:2 ratio of EDAC:NHS. The moduli of EDAC crosslinked collagen gels have been measured in our previous work as ranging between 0.01 (0 mM/mg) and 1 kPa (150 mM/mg) (6).

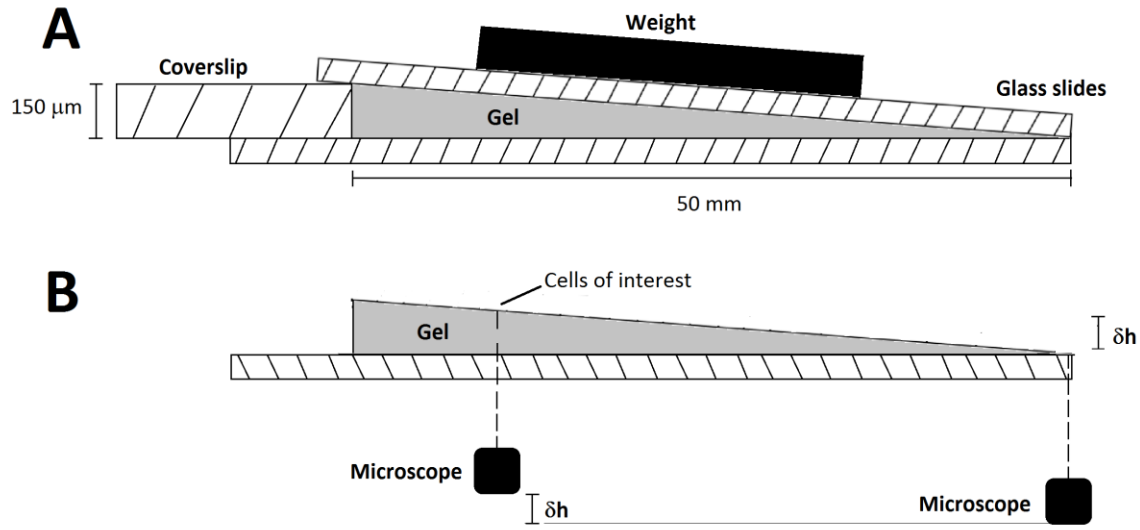

Figure 1: A) Schematic showing wedge shaped gel formation. Gels ranged from a height of 0 to 150 μm across a horizontal distance of 50 mm. **B)** Gel height was confirmed by recording the change in the vertical position of the microscope relative to the stage required to focus on the top surface of the gel.

Polyacrylamide gels were formed by varying the concentrations of acrylamide and bis-acrylamide to alter the gel stiffness as described previously (17), before being polymerised with 0.15% TEMED (Sigma Aldrich). Flat and wedge shaped polyacrylamide gels were formed between treated glass coverslips as described above. SulfoSANPAH (Fischer Scientific, Waltham MA), a heterobifunctional crosslinker was diluted to 1 mg/mL in HEPES buffer and used to bind acetic acid diluted collagen (2 mg/mL) to the gel surface to allow for cell attachment (28). Bulk gel moduli of similar polyacrylamide gels were ascertained from previous studies showing a range of moduli from 0.6 to 153 kPa (17).

Cell culture

MC3T3-E1 cells, an immortalised pre-osteoblast cell line were maintained in Alpha Modified Eagle's Medium (α-MEM) containing 100 ug/mL L-glutamine and supplemented with 10% foetal bovine serum and 100 U/mL Antibacterial-Antimytotic (all Sigma Aldrich). All experiments were conducted at passage 4. Cells were cultured on flat and wedge shaped gels of either polyacrylamide or collagen for 24 hours at 37 ˚C and 5% CO_2. Cells were then fixed with 4% paraformaldehyde. Membrane permeabilization was conducted with 0.1% Triton in

Phosphate Buffered Saline (PBS) (both Sigma Aldrich) and cells were stained with Fluorescein isothiocyanate (FITC) labelled rhodamine-phalloidin (to stain the actin cytoskeleton) and Hoechst (to stain cell nuclei) (both BD Biosciences, San Jose CA). Cells examined for ALP activity were culture for 7 days before being lysed.

Cell imaging

Cells were imaged using a Leica DM2700 inverted microscope at 10X magnification and the average cell spread area was quantified as a measure of osteogenic differentiation. Gel height at each location was verified by first focussing on the top surface of the glass slide, and then recording the vertical movement of the microscope stage required to focus on the cells of interest. This is further illustrated in Figure 1 B).

Osteogenic assays

Cells were lysed using Cellytic M with 1% protease inhibitor cocktail (both Sigma Aldrich). ALP activity was quantified using a colourimetric assay (Sigma Aldrich) as described previously [Mullen, 2013 #298][Birmingham, 2012 #247]. Results were then normalised to the DNA content of each well.

Finite element methods

Substrate Model generation

The materials under study are a type 1 collagen gel, the microstructure of which may be varied by chemical crosslinking, allowing a greater number of adjacent fibres to form zero length molecular bonds with one another, thus affecting the materials mechanical properties (29). To understand the role of microstructural crosslinking density on the mechanical response of these gels, a micromechanical model was developed using ABAQUS finite element software (Dassault Systemes, Vélizy-Villacoublay, France), representing the fibrous and non-fibrous phases of this material discretely within a finite element framework. This approach was used to predict the effective properties of random collagen fibre distributions, with a range of crosslinking densities to study their effect on macroscopic material behaviour.

The fibres within collagen gels exhibit no preferential orientation and can therefore be considered to be randomly oriented. They measure approximately 200 nm (30) in diameter and account for approximately 20% of the material volume fraction (31, 32). A numerical algorithm was developed to create representative distributions of these fibrous gels in two-dimensions, whereby each fibre was assigned a centre point, C, which was randomly chosen within a domain measuring 450 by 450 μm. The orientation of each fibre was also chosen to be a random angle θ, where $-\pi \geq \theta > \pi$. The fibre end points were then generated by extrapolating half the length (chosen randomly between the limits 10 and 500 μm) in the direction of the angle θ and its opposite angle θ-180. Fibres were then truncated so as to fall within the confines of the gel as appropriate. A resulting collagen fibre distribution generated using this procedure is shown in Figure 2(B). Models were generated for a range of crosslinking densities with crosslinked and non-crosslinked fibres being introduced to the model separately. Briefly, for each model, the relevant crosslinked fibres were imported to the ABAQUS sketch facility as a single part through a Python script. This created a series of fibres where each intersecting point was assigned a unique node, while a single element joined corresponding nodes to one another. Non-crosslinked fibres were introduced as discrete nodes and elements to the relevant Abaqus input file, with a single element spanning the entire length of each fibre. Thus non-crosslinked fibres were prevented from directly

interacting with one another, although indirect interaction between non-crosslinked fibres could still occur through the gel. This process was repeated for 5 different fibre permutations in order to minimise the effects of individual fibre location variation on the results.

Material Model

Plane stress finite element models were created to simulate a 100 μm wide section of a soft gel containing relatively stiff collagen fibres. Fibres were set as linear, tension only, truss elements (T2D2) with a circular cross-section of radius 100 nm and embedded into the plane stress element (CPS8R) gel region. A Young's modulus of 10 Pa was assigned to the gel based on previous atomic force microscopy measurements (6). A Young's modulus of 2 MPa was assigned to the fibres in order to achieve a range of equivalent stiffnesses on the same scale as the range present in the polyacrylamide substrates investigated.

Loading and Boundary Conditions to simulate cell contraction

Figure 2 A) shows a representation of a single cell interacting with the collagen fibres within an infinitely stiff and thick gel, situated on a glass slide. The cell interacts with the substrate through focal adhesion complexes, and can induce a contractile force on the gel. The resistance of the gel to this force, termed "equivalent shear stiffness" in this study, is interpreted by the cell and the force induced by the cell is altered until homeostasis is achieved. Figure 2 B) is the finite element approximation applied in this study to simulate the interaction between a contracting cell and a fibrous gel on a glass slide. The cell is not discretely modelled, but is represented by a nominal shear load of 1 N, acting at the edges of fibres, based on recent measurements for the dimensions of MC3T3-E1 cells on collagen gels (33). A no slip boundary condition is used to simulate the rigid coverslip under the gel, while a free slip boundary condition is used where symmetry exists in order to improve model efficiency. The horizontal movement of the nodes is used as a measure of the equivalent shear stiffness of the gel structure in response to the applied load.

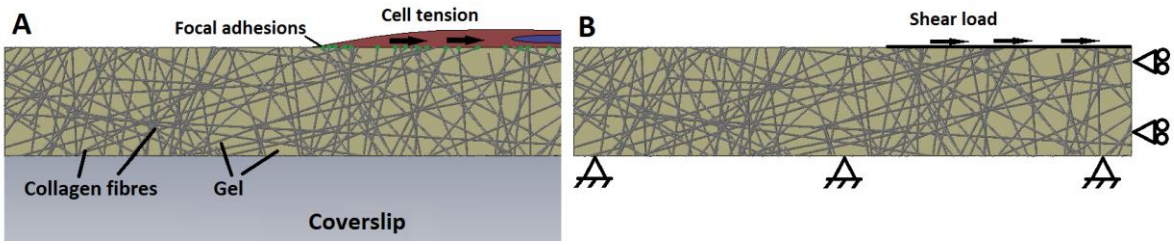

Figure 2: A) Schematic of an MC3T3-E1 cell applying force to a fibrous substrate. The force applied by the cell is transferred through the focal adhesion complexes and resisted by the gel. **B)** Boundary conditions placed on micromechanics model. A shear load of 1 N was applied to the nodes to simulate the forces exerted by the cell at the cell-substrate interface.

Statistical methods

A two way ANOVA was conducted to determine statistical significance in both the experimental and computational results.

Results

Experimental results

On flat gels of 0.6 or 1.2 kPa, cells adopt an encapsulated morphology and converge into groups as shown in Figure 3 (A). The average cell spread area on these substrates is 400 μm^2. Above this stiffness cells separate from one another and begin to elongate, increasing their area to between 700 and 800 μm^2 on substrates of between 2.4 kPa and 9.6 kPa, as shown in Figure 3 (G). The cells do not group together on these substrates as demonstrated by the dispersed nature of the cells in Figure 3 (B). On stiffer substrates (19.6 kPa and above), cells increase their area to an average of between 1200 and 1600 μm^2 and adopt the spread morphology associated with osteoblasts, see Figure 3 (C). It was also observed that the cells exhibited a larger area on thin polyacrylamide gels, with cells cultured on a wedge shaped 1.2 kPa gel having an average area of 1380 ± 644 μm^2 and 830 ± 341 μm^2 on a 1 μm and 3 μm thick section of the gel respectively. However, as shown in Figure 4, gel depth had no effect on cell area above 5 μm.

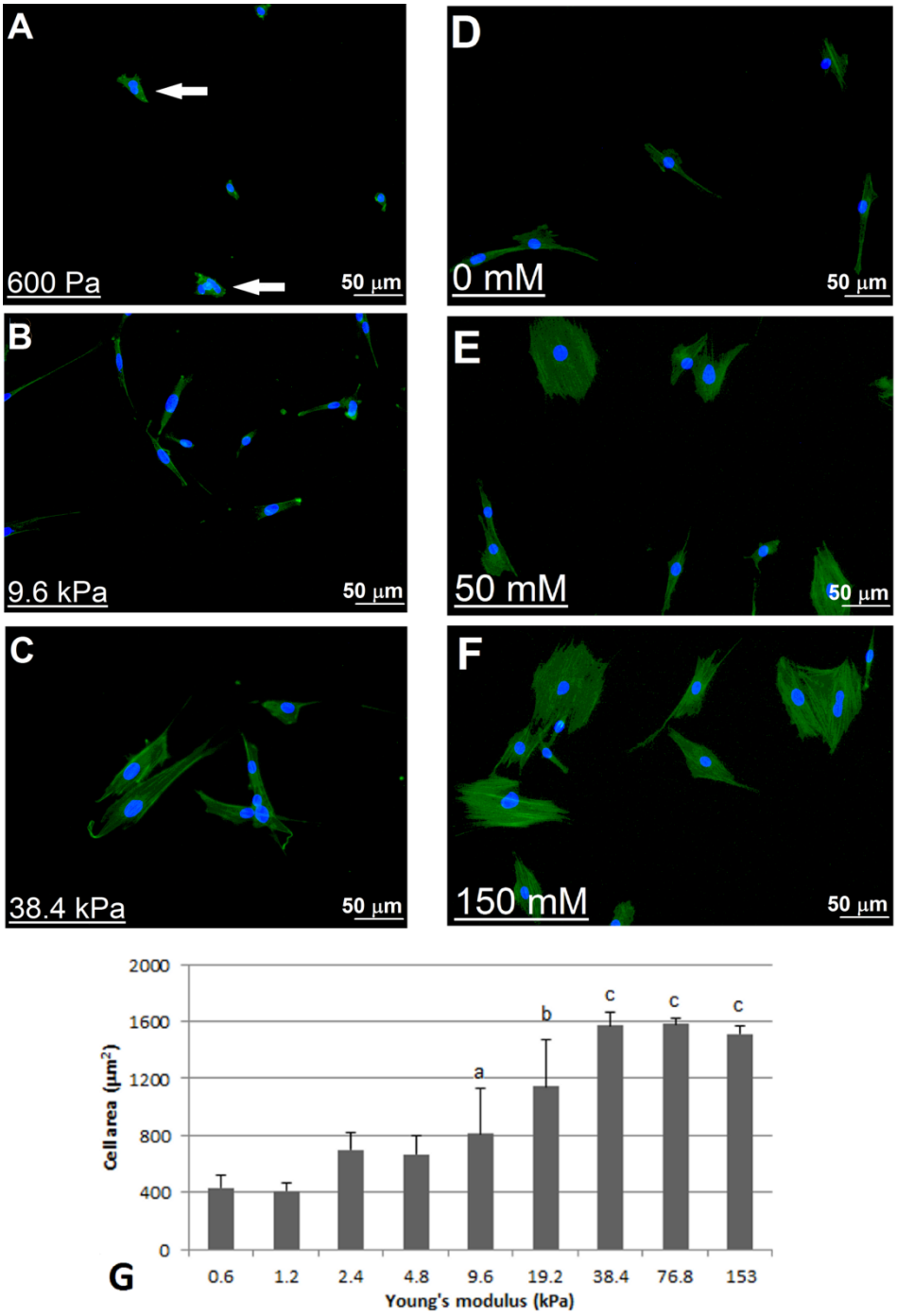

Figure 3: Representative images of MC3T3-E1 cells on polyacrylamide gels of: A) 600 Pa, B)_9.6 kPa and C) 38.4 kPa and Collagen gels crosslinked with: D) 0mM EDAC, E) 50 mM EDAC and F) 150 mM EDAC. White arrows on A) indicate multiple cells grouped together; and G) Cell spread area of MC3T3-E1 cells cultured on polyacrylamide gels of approx. 70 µm. **a** indicates statistically higher than 0.6 kPa to 4.8 kPa gels. **b** indicates statistically higher than 0.6 kPa to 9.6 kPa gels. **c** indicates statistically higher than 0.6 kPa to 19.2 kPa gels. $p < 0.05$.

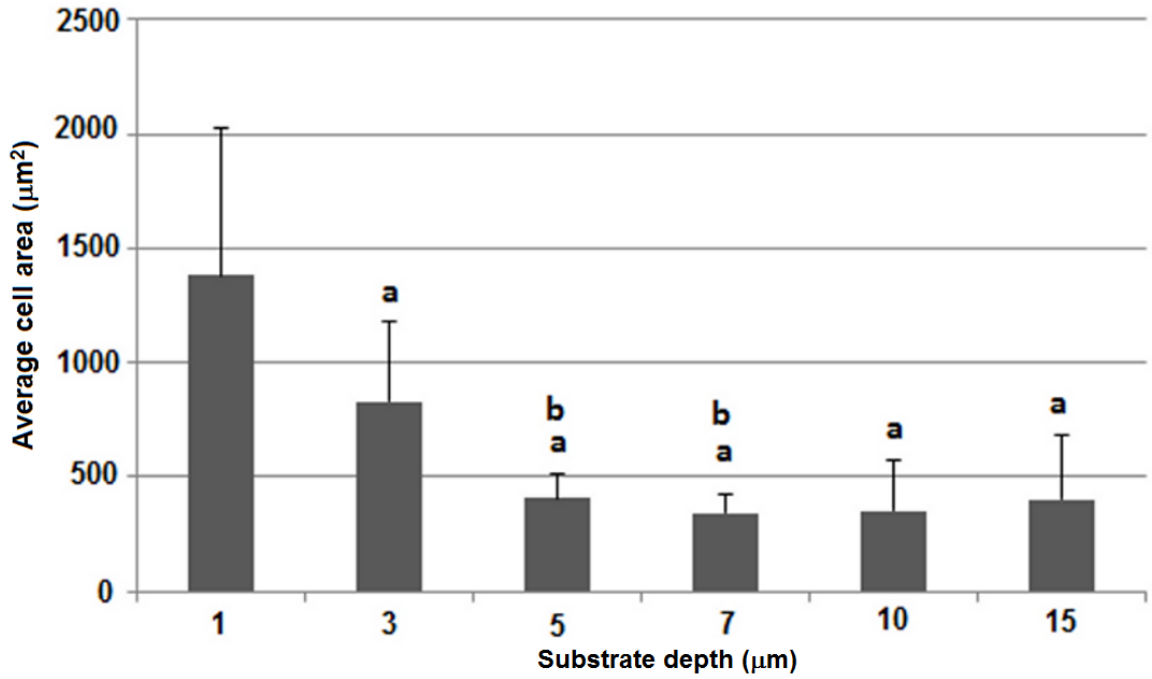

Figure 4: Cell spread area of MC3T3-E1 cells cultured on wedge shaped soft (1.2 kPa) polyacrylamide gels of various thicknesses. **a** indicates statistically difference to cells cultured on 1 μm thick gel. **b** indicates statistically difference to cells cultured on 3 μm thick gel. $p < 0.05$.

Cell area on crosslinked collagen substrates increased as the crosslinking density was increased. As shown in Figure 3 G), the lowest average spread area is 478 ± 214 μm^2, which occurred on the non-crosslinked gel (shown in Figure 3 (D)), where the cells typically display an elongated morphology, similar to that observed on the 9.6 kPa PA gel, shown in Figure 3 (B). On gels with a higher density of crosslinking (50 to 150 mM/mg collagen (Figures 3 (E) and 3 (F)), the cells adopt the spread morphology as observed on 38.4 kPa PA gels, shown in Figure 3 (C), while the average spread cell area increases to between 1200 μm^2 and 1600 μm^2. Cell spread area was also shown to increase as the gel thickness was decreased, and this effect was more pronounced on gels with a low crosslinking density. As shown in Figure 5, a large rise in cell area, from 389 ± 54 μm^2 to 1478 ± 283 μm^2 was observed as the thickness of a non-crosslinked collagen gel was decreased from 150 μm to 5 μm. On more densely crosslinked gels (50 to 150 mM EDAC), the thickness of the structure had less effect on the spread cell area. This is also shown in Figure 5, where the average cell spread area on 150 mM EDAC-crosslinked gels increases from 1451 ± 132 μm^2 to 1761 ± 247 μm^2.

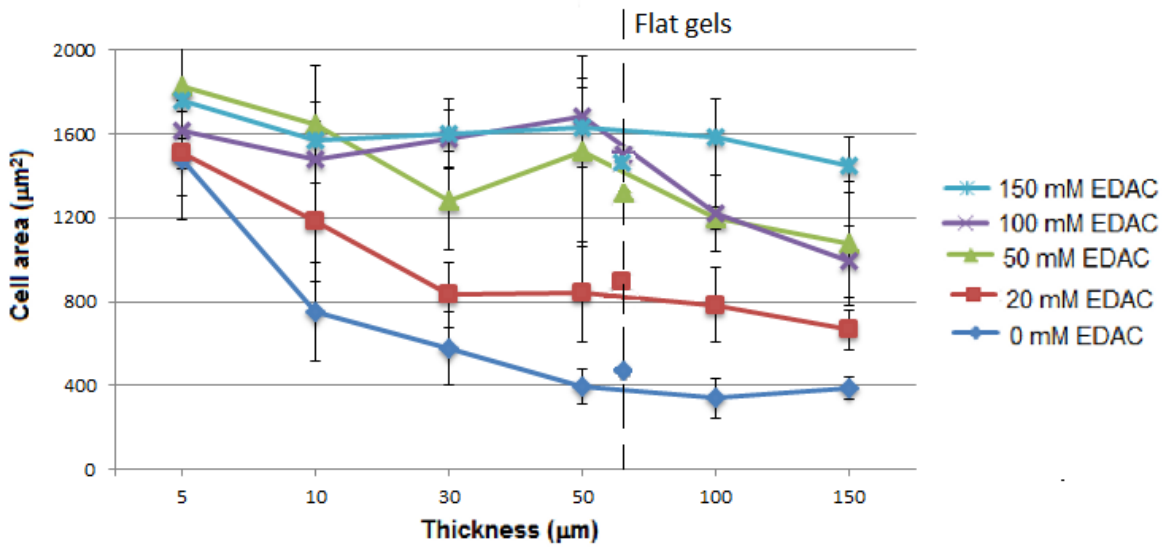

Figure 5: Cell Area (μm^2) of MC3T3-E1 cells cultured on wedge shaped crosslinked collagen substrates. The average cell area at relevant thickness for each gel is presented. The average cell area on flat gels (approx. 70 µm thick) are presented the respective markers for each concentration of crosslinking agent.

As shown in Figure 6 (A), ALP activity was shown to be present on all collagen gels of lower with levels of between 1.4 ± 0.18 mM/ng DNA and 1.1.7 ± 0.14 mM/ng DNA. In cells cultured on PA gels, the highest levels of ALP activity (between 1.04 and 1.16 mM/ng DNA) was found in cells cultured on gels of above 19.6 kPa (see Figure 6 (B)). Cells cultured on softer gels exhibited lower levels of ALP activity of between 0.04 and 0.4 mM/ng DNA.

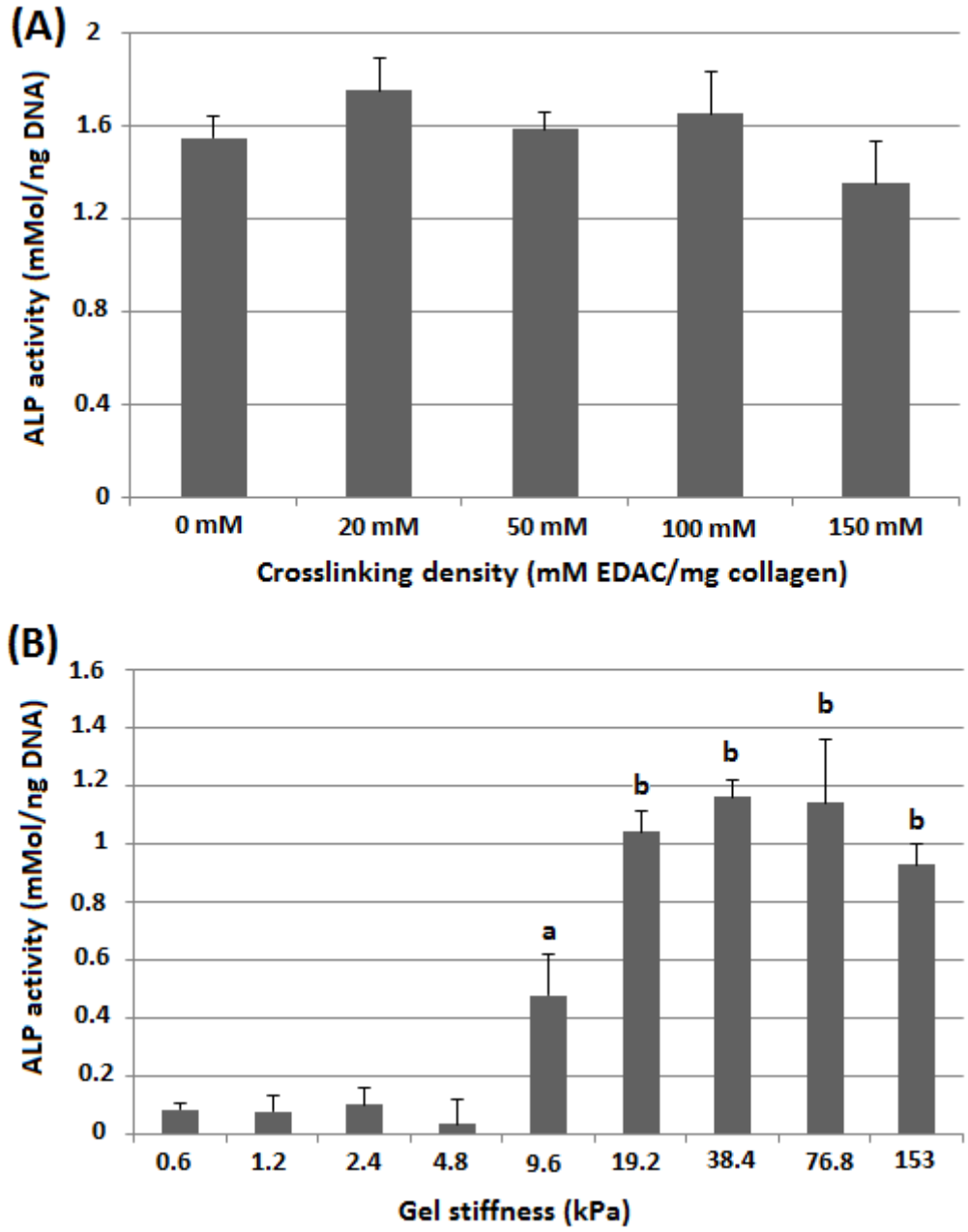

Figure 6: ALP activity normalised to DNA content measured in cells cultured on **(A)** collagen gels and **(B)** polyacrylamide gels for 7 days in expansion media. **a** indicates significantly higher activity than cells cultured on PA gels of 4.8 kPa and below. **b** indicates significantly higher activity than cells cultured on PA gels of 9.6 kPa and below. $p < 0.05$.

Finite element results

Figure 7 shows the average horizontal motion of the nodes subjected to a 1 N load (representing cell contraction) for both the fibrous gel models and non-fibrous gels of various Young's moduli. The motion of these nodes was used as an indicator of the equivalent shear

stiffness of the substrates. The equivalent stiffness of non-fibrous polyacrylamide gels decreased linearly as gel modulus was increased. It was also seen that a logarithmic increase in equivalent stiffness occurred as gel thickness was reduced, with the motion recorded in a 10kPa gel reduced from 0.88 nm in a 150 μm to 0.6 pm in a 1 μm gel. It was observed that the introduction of fibres to the gel greatly increased the equivalent stiffness of the substrates, with fibrous gels showing similar levels of motion to non-fibrous gels with Young's moduli of between 5 and 20 kPa. For fibrous gels, the motion of the nodes increased from 2.86 nm to 0.36 nm as the percentage of crosslinked fibres was increased from 0 to 100% in a 150 μm gel, indicating an increase in the equivalent stiffness. A decrease in gel thickness also increased the equivalent stiffness of the gels, although this effect was stronger in gels with a lower percentage of crosslinked fibres. This can be seen most clearly in Figure 7 where the motion observed in the non-crosslinked gel decreases from 2.86 nm to 0.42 nm as the gel thickness is decreased from 150 μm to 10 μm, while the fully crosslinked gel experience a decrease in motion from 0.36 nm to 0.21 nm over the same decrease in thickness.

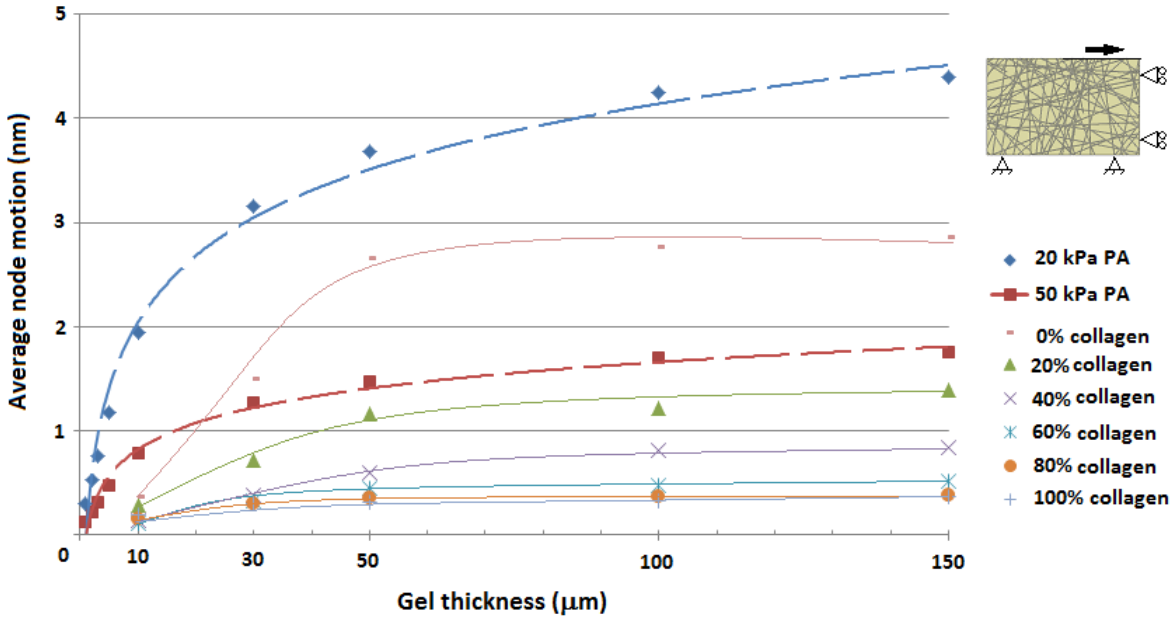

Figure 7: Equivalent shear stiffness of non fibrous polyacrylamide and fibrous crosslinked collagen gels of different thicknesses as calculated using ABAQUS software.

The motion experienced by these nodes in a fully crosslinked gel ranges from 0.21 nm at a depth of 10 μm, to 0.36 nm at a depth of 150 μm. This is similar to the level of motion experienced in a non-fibrous gel of 20 kPa. As the percentage of crosslinked fibres in the gel is decreased, the motion undergone by these nodes increases to as high as 2.8 nm for a gel containing no crosslinks between fibres at a depth of 150 μm.

Figure 8 shows the transfer of force through the fibrous gel in the non-crosslinked and fully crosslinked configurations. It can be observed that in the non-crosslinked gel force is borne mainly by the fibres which extend through the entire gel depth, while in the fully crosslinked gel force is transferred between fibres and so a greater percentage of fibres become involved in the mechanical resistance of the gel.

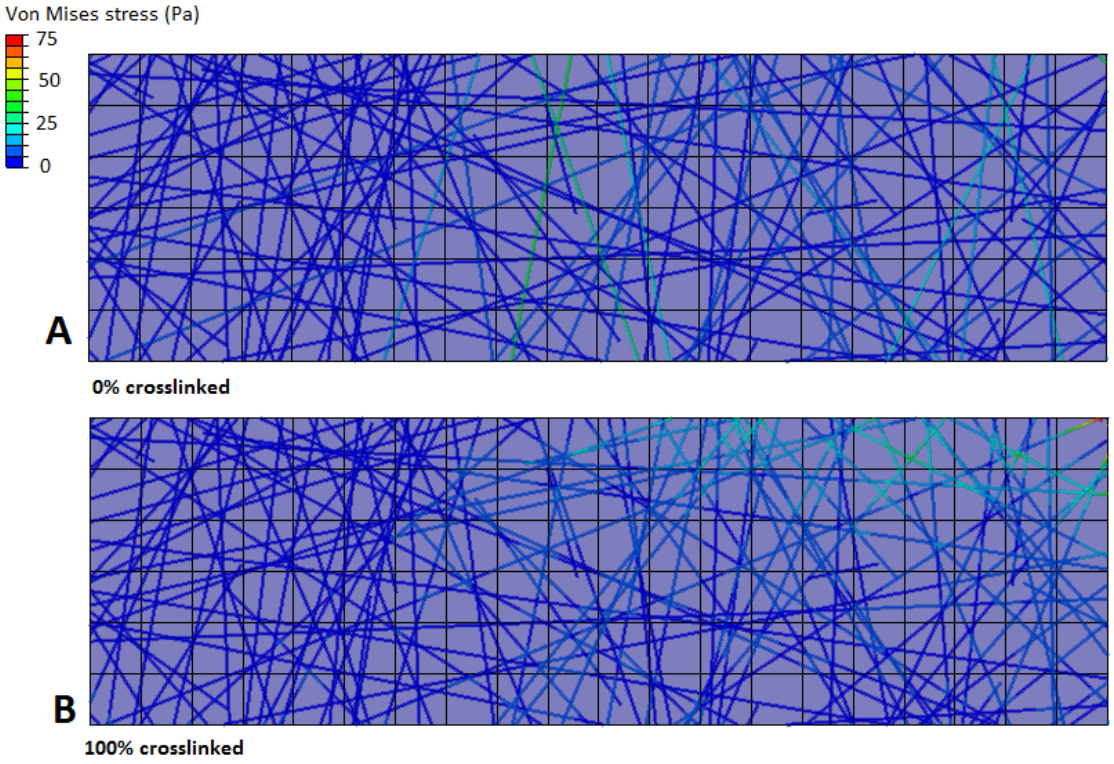

Figure 8: Force is transferred mainly through the fibres which span the entire gel depth in a non-crosslinked fibrous gel (A), while force is transferred through multiple adjoined fibres in a fully crosslinked gel (B).

Discussion

Cell spread area has been previously been shown to be an indicator of the differentiation stage of MSCs, with osteoblast differentiation found to correlate with increased cell area (34, 35). The results of this study demonstrate that cells on non-fibrous PA gels exhibited a larger spread cell area (>1600 μm^2) on stiffer gels (E>38 kPa). It was also shown that cells cultured on soft (Young's modulus < 300 Pa) fibrous collagen substrates exhibit the same large spread area (1200-1600 μm^2) as those cultured on stiff (E>38 kPa) PA gels. Moreover, as the concentration of crosslinking agent used in these firous gels was increased, the cell spread area also increased. The finite element studies conducted here predict that the equivalent shear stiffness of a fibre-reinforced soft gel is significantly greater than that of a non fibrous gel. It was also shown that, at high crosslinking concentrations (100% of fibres crosslinked), the effective stiffness experienced by the cells approached that experienced by cells on much stiffer non-fibrous substrates. These results provide an insight into why cell spread area on crosslinked collagen gels, which are very soft (<1 kPa) when measured through nanoindentation, is akin to that of cells cultured on much stiffer non-fibrous gels. Gel thickness was also shown to have an effect on both cell spread area and effective stiffness. Experimental results showed that thinner substrates resulted in an increase in cell spread area, while the computational simulations revealed that such results could be related to an increase in effective stiffness as gel thickness was reduced. However, it was noted that effect of gel thickness was less for cells plated on highly crosslinked collagen gels.

A possible limitation of this study is the use of the MC3T3-E1 cell line as a model of primary osteoblasts. However, these cells have been shown to be a suitable model for several aspects of osteoblast behaviour, including ALP expression and matrix mineralisation (36, 37), while they have also been used to investigate cell spread area in response to substrate stiffness (38). (Another possible limitation is that cell differentiation was not directly measured but inferred from cell spread area. However, tensile testing has shown that osteoblasts change the mechanical properties of their substrate over time (39). This increase in stiffness is due to matrix mineralisation and is a vital part of the differentiation process, thus examination of the exact stimuli experienced by the cell is not possible once the cells have begun to differentiate. Further to this, cell area immediately after plating has been shown to be a good predictor of osteogenic differentiation of MSCs after 7 and 21 days culture (34).)

The effects of substrate modulus and thickness on cell behaviour have both been studied in detail previously (5, 21, 24). However, the interplay between the various factors, i.e. bulk modulus, thickness and in particular material microstructure, has yet to be elucidated. The results presented in this study provide an insight into bone cell behaviour and provide a possible explanation for previous contradictions concerning the differentiation of osteogenic cells in response to extracellular matrix stiffness (5, 18, 40). Specifically it has been shown that the combined effects of substrate modulus, thickness and microstructure must be taken into account in order to determine the mechanical forces experienced at the cellular level.

Gel crosslinking has been widely used a method of altering the stiffness of substrates and scaffolds used in in vitro experiments (6, 14, 29). An advantage of the method is that the surface chemistry can remain constant while the mechanical properties of the gel are altered. However, as of yet the interaction between gel crosslinking and the thickness of the substrate has not been investigated. In this study it is shown that a highly crosslinked collagen gel can reduce the effect of gel thickness on cell area. Gel thickness has also been shown to affect cell behaviour to different extents depending on the nature of the gel material, with cells on fibrous materials being influenced by gel thicknesses of up to over 130 μm (20), while cells on non-fibrous materials are only influenced by structures within 5-10 μm of the cell (21, 22). The results of this study further illustrate that the effect of gel thickness on cell area is dependent on the microstructure of the gel, specifically the presence of discrete fibres and the interaction present between those fibres (crosslinking density).

To understand the mechanisms behind this behaviour the results of the finite element micromechanical simulations presented here must be considered. These simulations demonstrate that the effective shear stiffness, a measure of the stiffness as experienced by the cell, of a non-fibrous gel was increased as the gel thickness is decreased. This is because in a thin gel, the stiffness as experienced by the cell is dominated by the comparatively stiff underlying coverslip (21, 22). The models also showed that in fibrous gels, such as the collagen gels investigated in this study, contractile forces from the cell were predominantly transferred through the fibres rather than through the remainder of the gel. Specifically it was shown that fibres that spanned the entire depth of the gel transferred the majority of the force. This provides an explanation for the increase in cell spread area on thinner collagen gels, due to a larger number of fibres extending through the entire depth of a thinner gel. It was also shown that there was a very slight increase in equivalent stiffness as the gels became thinner when all of the fibres in the gel were joined through crosslinks, which corresponds to the reduced effect of gel thickness on cell spread area on highly crosslinked collagen gels. This can be explained by the high level of crosslinking between the fibres which allows force to be

transferred through multiple fibres through the entire gel depth, in a way allowing multiple connected fibres to behave as one larger fibre. This in turn increases the equivalent stiffness of the gels and therefore the spread area of cells cultured on these gels.

These results have important implications for the development of future tissue engineering strategies. Specifically, they demonstrate that the material properties measured through commonly used techniques such as AFM (5, 41), nanoindentation (42, 43) and confined/unconfined compression (44, 45) may not reflect the mechanical stimulation experienced at the cellular level. This is of particular significance when investigating fibrous materials, such as those commonly used in bone tissue engineering strategies (14, 46, 47). The results presented here highlight the fact that greater attention must be paid to the effects of the local mechanical environment (i.e. cellular level) if further advances are to be made in the field of bone tissue engineering.

Conclusion

To the author's knowledge, this is the first time the combined effects of substrate modulus, thickness and microstructure on cell behaviour have been investigated and this study provides an enhanced understanding of the forces actually experienced by osteogenic cells in 2D in-vitro experiments. The results presented here demonstrate that commonly utilised methods of substrate modulus measurement cannot accurately interpret the overall stiffness as experienced by the cell. Future studies should consider the substrate modulus, thickness and micromechanical structure during comparison of cell behaviour on different substrates. The findings in this study can improve the current understanding of osteogenic mechanotransduction and pave the way for a more successful transfer of in-vitro experimental findings to tissue regeneration strategies.

References

1. Tanaka Kamioka, K., H. Kamioka, H. Ris, and S.-S. Lim. 1998. Osteocyte Shape Is Dependent on Actin Filaments and Osteocyte Processes Are Unique Actin-Rich Projections. Journal of Bone and Mineral Research 13:1555-1568.
2. Bonewald, L. F. 2011. The amazing osteocyte. Journal of Bone and Mineral Research 26:229-238.
3. Kapur, S., D. J. Baylink, and W. K. H. Lau. 2003. Fluid flow shear stress stimulates human osteoblast proliferation and differentiation through multiple interacting and competing signal transduction pathways. Bone 32:241-251.
4. You, L., S. Temiyasathit, P. Lee, C. H. Kim, P. Tummala, W. Yao, W. Kingery, A. M. Malone, R. Y. Kwon, and C. R. Jacobs. 2008. Osteocytes as mechanosensors in the inhibition of bone resorption due to mechanical loading. Bone 42:172-179.
5. Engler, A. J., S. Sen, H. L. Sweeney, and D. E. Discher. 2006. Matrix Elasticity Directs Stem Cell Lineage Specification. Cell 126:677-689.
6. Mullen, C. A., M. G. Haugh, M. B. Schaffler, R. J. Majeska, and L. M. McNamara. 2013. Osteocyte differentiation is regulated by extracellular matrix stiffness and intercellular separation. Journal of the Mechanical Behavior of Biomedical Materials 28:183-194.
7. Ponik, S. M., J. W. Triplett, and F. M. Pavalko. 2007. Osteoblasts and osteocytes respond differently to oscillatory and unidirectional fluid flow profiles. Journal of Cellular Biochemistry 100:794-807.
8. Weyts, F. A. A., B. Bosmans, R. Niesing, J. P. T. M. Leeuwen, and H. Weinans. 2003. Mechanical Control of Human Osteoblast Apoptosis and Proliferation in Relation to Differentiation. Calcified Tissue International 72:505-512.
9. Papachroni, K. K., D. N. Karatzas, K. A. Papavassiliou, E. K. Basdra, and A. G. Papavassiliou. 2009. Mechanotransduction in osteoblast regulation and bone disease. Trends in Molecular Medicine 15:208-216.
10. Santos, A., A. D. Bakker, and J. Klein-Nulend. 1999. The role of osteocytes in bone mechanotransduction. Osteoporosis International 20:1027-1031.
11. Keogh, M. B., F. J. O'Brien, and J. S. Daly. 2010. Substrate stiffness and contractile behaviour modulate the functional maturation of osteoblasts on a collagen-GAG scaffold. Acta Biomaterialia 6:4305-4313.
12. Tsai, S. W., H. M. Liou, C. J. Lin, K. L. Kuo, Y. S. Hung, R. C. Weng, and F. Y. Hsu. 2012. MG63 Osteoblast-Like Cells Exhibit Different Behavior when Grown on Electrospun Collagen Matrix versus Electrospun Gelatin Matrix. PLoS ONE 7:e31200.
13. Evans, N. D., C. Minelli, E. Gentleman, V. LaPointe, S. N. Patankar, M. Kallivretaki, X. Chen, C. J. Roberts, and M. M. Stevens. 2009. Substrate stiffness affects early differentiation events in embryonic stem cells.
14. Tierney, C. M., M. G. Haugh, J. Liedl, F. Mulcahy, B. Hayes, and F. J. O'Brien. 2009. The effects of collagen concentration and crosslink density on the biological, structural and mechanical properties of collagen-GAG scaffolds for bone tissue engineering. Journal of the Mechanical Behavior of Biomedical Materials 2:202-209.
15. Chau, D. Y., R. J. Collighan, E. A. M. Verderio, V. L. Addy, and M. Griffin. 2005. The cellular response to transglutaminase-cross-linked collagen. Biomaterials 26:6518-6529.
16. Wang, Y. L., and R. J. Pelham Jr. 1998. [39] Preparation of a flexible, porous polyacrylamide substrate for mechanical studies of cultured cells. In Methods in Enzymology. B. V. Richard, editor. Academic Press. 489-496.
17. Tse, J. R., and A. J. Engler. 2001. Preparation of Hydrogel Substrates with Tunable Mechanical Properties. In Current Protocols in Cell Biology. John Wiley & Sons, Inc.

18. Khatiwala, C. B., S. R. Peyton, and A. J. Putnam. 2006. Osteogenic Differentiation of Mc3t3-E1 Cells Regulated by Substrate Stiffness Requires Mapk Activation. In Cell Adhesion and Migration.
19. Dalby, M. J., N. Gadegaard, R. Tare, A. Andar, M. O. Riehle, P. Herzyk, C. D. W. Wilkinson, and R. O. C. Oreffo. 2007. The control of human mesenchymal cell differentiation using nanoscale symmetry and disorder. Nature materials 6:997-1003.
20. Leong, W. S., C. Y. Tay, H. Yu, A. Li, S. C. Wu, D. H. Duc, C. T. Lim, and L. P. Tan. 2010. Thickness sensing of hMSCs on collagen gel directs stem cell fate. Biochemical and Biophysical Research Communications 401:287-292.
21. Sen, S., A. Engler, and D. Discher. 2009. Matrix Strains Induced by Cells: Computing How Far Cells Can Feel. Cel. Mol. Bioeng. 2:39-48.
22. Maloney, J. M., E. B. Walton, C. M. Bruce, and K. J. Van Vliet. 2008. Influence of finite thickness and stiffness on cellular adhesion-induced deformation of compliant substrata. Physical Review E 78:041923.
23. Feng, C. H., Y. C. Cheng, and P. H. G. Chao. 2013. The influence and interactions of substrate thickness, organization and dimensionality on cell morphology and migration. Acta Biomaterialia 9:5502-5510.
24. Rudnicki, M. S., H. A. Cirka, M. Aghvami, Edward A. Sander, Q. Wen, and Kristen L. Billiar. 2013. Nonlinear Strain Stiffening Is Not Sufficient to Explain How Far Cells Can Feel on Fibrous Protein Gels. Biophys. J. 105:11-20.
25. Ma, X., M. E. Schickel, Mark D. Stevenson, Alisha L. Sarang Sieminski, Keith J. Gooch, Samir N. Ghadiali, and Richard T. Hart. 2013. Fibers in the Extracellular Matrix Enable Long-Range Stress Transmission between Cells. Biophys. J. 104:1410-1418.
26. Stylianopoulos, T., and V. H. Barocas. 2007. Volume-averaging theory for the study of the mechanics of collagen networks. Computer Methods in Applied Mechanics and Engineering 196:2981-2990.
27. Chandran, P. L., Barocas VH. 2007. Deterministic material-based averaging theory model of collagen gel micromechanics. J Biomech Eng 129:137-147.
28. Fischer, R. S., K. A. Myers, M. L. Gardel, and C. M. Waterman. 2012. Stiffness-controlled three-dimensional extracellular matrices for high-resolution imaging of cell behavior. Nature protocols 7:2056-2066.
29. Haugh, M. G., C. M. Murphy, R. C. McKiernan, C. Altenbuchner, and F. J. O'Brien. 2011. Crosslinking and Mechanical Properties Significantly Influence Cell Attachment, Proliferation, and Migration Within Collagen Glycosaminoglycan Scaffolds. Tissue Engineering Part A 17:1201-1208.
30. McDaniel, D. P., G. A. Shaw, J. T. Elliott, K. Bhadriraju, C. Meuse, K.-H. Chung, and A. L. Plant. 2007. The Stiffness of Collagen Fibrils Influences Vascular Smooth Muscle Cell Phenotype. Biophys. J. 92:1759-1769.
31. Saidi, I. S., S. L. Jacques, and F. K. Tittel. 1995. Mie and Rayleigh modeling of visible-light scattering in neonatal skin. Appl. Opt. 34:7410-7418.
32. Driessen, N. J. B., G. W. M. Peters, J. M. Huyghe, C. V. C. Bouten, and F. P. T. Baaijens. 2003. Remodelling of continuously distributed collagen fibres in soft connective tissues. Journal of Biomechanics 36:1151-1158.
33. Mullen, C. A., T. J. Vaughan, M. C. Voisin, M. A. Brennan, P. Layrolle, and L. M. McNamara. 2014. Cell morphology and focal adhesion location alters internal cell stress. Journal of The Royal Society Interface 11.
34. Song, W., N. Kawazoe, and G. Chen. 2011. Dependence of Spreading and Differentiation of Mesenchymal Stem Cells on Micropatterned Surface Area. Journal of Nanomaterials 2011.
35. Kilian, K. A., B. Bugarija, B. T. Lahn, and M. Mrksich. 2010. Geometric cues for directing the differentiation of mesenchymal stem cells. Proceedings of the National Academy of Sciences 107:4872-4877.

36. Quarles, L. D., D. A. Yohay, L. W. Lever, R. Caton, and R. J. Wenstrup. 1992. Distinct proliferative and differentiated stages of murine MC3T3-E1 cells in culture: An in vitro model of osteoblast development. Journal of Bone and Mineral Research 7:683-692.
37. Sudo, H., H. A. Kodama, Y. Amagai, S. Yamamoto, and S. Kasai. 1983. In vitro differentiation and calcification in a new clonal osteogenic cell line derived from newborn mouse calvaria. The Journal of Cell Biology 96:191-198.
38. Khatiwala, C. B., S. R. Peyton, and A. J. Putnam. 2006. Intrinsic mechanical properties of the extracellular matrix affect the behavior of pre-osteoblastic MC3T3-E1 cells. American Journal of Physiology - Cell Physiology 290:C1640-C1650.
39. Buxton, P. G., M. Bitar, K. Gellynck, M. Parkar, R. A. Brown, A. M. Young, J. C. Knowles, and S. N. Nazhat. 2008. Dense collagen matrix accelerates osteogenic differentiation and rescues the apoptotic response to MMP inhibition. Bone 43:377-385.
40. Rowlands, A. S., P. A. George, and J. J. Cooper-White. 2008. Directing osteogenic and myogenic differentiation of MSCs: interplay of stiffness and adhesive ligand presentation. American Journal of Physiology - Cell Physiology 295:C1037-C1044.
41. Huang, C., P. J. Butler, S. Tong, H. S. Muddana, G. Bao, and S. Zhang. 2013. Substrate Stiffness Regulates Cellular Uptake of Nanoparticles. Nano Letters 13:1611-1615.
42. Lahiri, D., A. P. Benaduce, F. Rouzaud, J. Solomon, A. K. Keshri, L. Kos, and A. Agarwal. 2011. Wear behavior and in vitro cytotoxicity of wear debris generated from hydroxyapatite–carbon nanotube composite coating. Journal of Biomedical Materials Research Part A 96A:1-12.
43. Mante, F. K., G. R. Baran, and B. Lucas. 1999. Nanoindentation studies of titanium single crystals. Biomaterials 20:1051-1055.
44. Haugh, M. G., M. J. Jaasma, and F. J. O'Brien. 2009. The effect of dehydrothermal treatment on the mechanical and structural properties of collagen-GAG scaffolds. Journal of Biomedical Materials Research Part A 89A:363-369.
45. Bitar, M., V. Salih, R. Brown, and S. Nazhat. 2007. Effect of multiple unconfined compression on cellular dense collagen scaffolds for bone tissue engineering. Journal of Materials Science: Materials in Medicine 18:237-244.
46. Keogh, M., F. O' Brien, and J. Daly. 2010. A novel collagen scaffold supports human osteogenesis—applications for bone tissue engineering. Cell and Tissue Research 340:169-177.
47. Kim, H. W., J. C. Knowles, and H. E. Kim. 2005. Hydroxyapatite porous scaffold engineered with biological polymer hybrid coating for antibiotic Vancomycin release. Journal of Materials Science: Materials in Medicine 16:189-195.